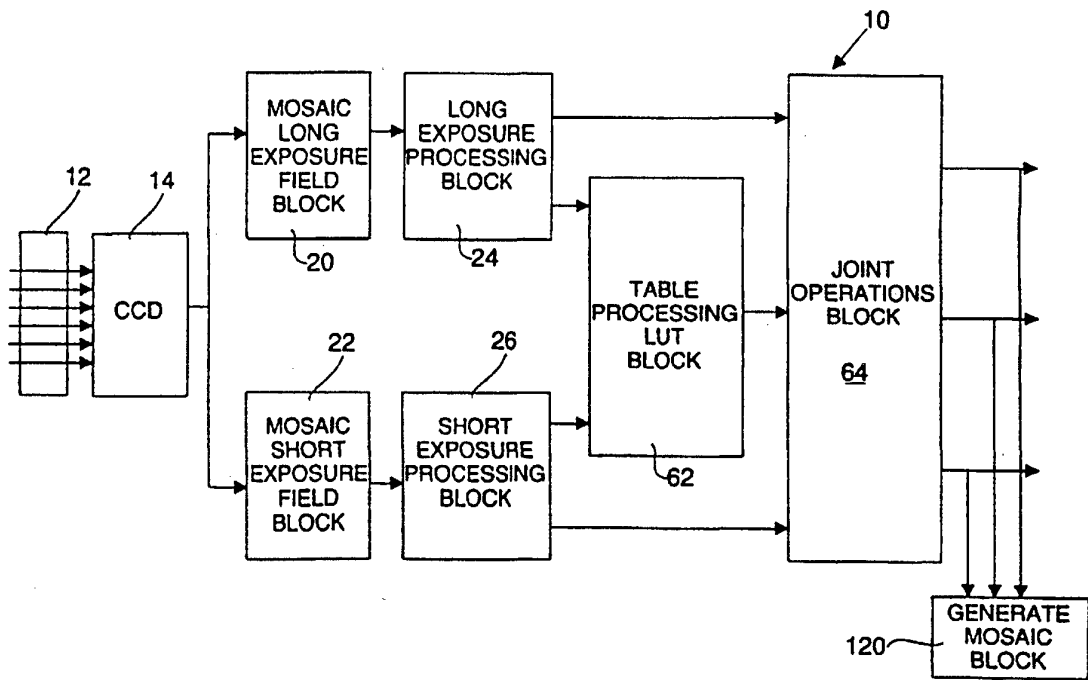




INTERNATIONAL APPLICATION PUBLISHED UNDER THE PATENT COOPERATION TREATY (PCT)

<p>(51) International Patent Classification <sup>5</sup> : H04N 9/07, 9/04, 5/228</p>	<p>A1</p>	<p>(11) International Publication Number: WO 94/18801 (43) International Publication Date: 18 August 1994 (18.08.94)</p>
<p>(21) International Application Number: PCT/US94/01358 (22) International Filing Date: 7 February 1994 (07.02.94) (30) Priority Data: 08/014,545 8 February 1993 (08.02.93) US (71) Applicant: I SIGHT, INC. [US/US]; 14 Ridgedale Avenue, Suite 125, Cedar Knolls, NJ 07927 (US). (72) Inventors: GINOSAR, Ran; Nofit (IL). GENOSSAR, Tamar; 20 Fichman Street, Haifa (IL). ZINATY, Ofra; 16/12 Peretz Markish Street, Haifa (IL). SOREK, Noam; Kiryat Haroshet (IL). KLIGLER, Daniel, J.; Moshav Zippori (IL). ZEEVI, Yehoshua, Y.; 48 Alexander Yannai Street, Haifa (IL). NEYSHTADT, Arkadi; 86-5 Shoshanat Hacarnel Street, Haifa (IL). AVNI, Dov; 7 Sukkot Street, Haifa (IL). (74) Agent: DIPPERT, William, H.; Cowan, Liebowitz &amp; Latman, 605 Third Avenue, New York, NY 10158 (US).</p>	<p>(81) Designated States: JP, European patent (AT, BE, CH, DE, DK, ES, FR, GB, GR, IE, IT, LU, MC, NL, PT, SE).  Published With international search report.</p>	

(54) Title: COLOR WIDE DYNAMIC RANGE CAMERA USING A CHARGE COUPLED DEVICE WITH MOSAIC FILTER



(57) Abstract

The apparatus (10) is a color wide dynamic range apparatus which includes a filter (12) interposed immediately in front of reoccurring color elements so that each pixel represents a given color element for the scene. At least two exposure levels are taken of the scene and the pixel outputs are decoded to generate the video luminance and chrominance signals. The images of the at least two exposure levels are combined to form a final image.

*FOR THE PURPOSES OF INFORMATION ONLY*

Codes used to identify States party to the PCT on the front pages of pamphlets publishing international applications under the PCT.

AT	Austria	GB	United Kingdom	MR	Mauritania
AU	Australia	GE	Georgia	MW	Malawi
BB	Barbados	GN	Guinea	NE	Niger
BE	Belgium	GR	Greece	NL	Netherlands
BF	Burkina Faso	HU	Hungary	NO	Norway
BG	Bulgaria	IE	Ireland	NZ	New Zealand
BJ	Benin	IT	Italy	PL	Poland
BR	Brazil	JP	Japan	PT	Portugal
BY	Belarus	KE	Kenya	RO	Romania
CA	Canada	KG	Kyrgystan	RU	Russian Federation
CF	Central African Republic	KP	Democratic People's Republic of Korea	SD	Sudan
CG	Congo	KR	Republic of Korea	SE	Sweden
CH	Switzerland	KZ	Kazakhstan	SI	Slovenia
CI	Côte d'Ivoire	LI	Liechtenstein	SK	Slovakia
CM	Cameroon	LU	Luxembourg	SN	Senegal
CN	China	LK	Sri Lanka	TD	Chad
CS	Czechoslovakia	LV	Latvia	TG	Togo
CZ	Czech Republic	MC	Monaco	TJ	Tajikistan
DE	Germany	MD	Republic of Moldova	TT	Trinidad and Tobago
DK	Denmark	MG	Madagascar	UA	Ukraine
ES	Spain	ML	Mali	US	United States of America
FI	Finland	MN	Mongolia	UZ	Uzbekistan
FR	France			VN	Viet Nam
GA	Gabon				

**COLOR WIDE DYNAMIC RANGE CAMERA  
USING A CHARGE COUPLED DEVICE WITH MOSAIC FILTER**

**CROSS-REFERENCE TO RELATED APPLICATIONS**

This application is a continuation-in-part of U.S. patent application Serial No. 07/795,350 filed November 20, 1991 entitled "Color Wide Dynamic Range Camera", which is, in turn, a continuation-in-part of U.S. patent application Serial No. 07/388,547, filed August 23, 1989, now U.S. Patent No. 5,114,442. Additionally, this application is related to U.S. Patent No. 4,858,014 and currently pending U.S. patent application Serial No. 07/805,512, filed December 11, 1991. The disclosures of all of the above-identified U.S. patents and patent applications are incorporated herein by reference.

**BACKGROUND OF THE INVENTION**

15

**Field of the Invention**

This invention pertains to video imagery and more particularly to apparatuses and techniques for providing enhancement of video color images. In particular, the present invention uses a four-color mosaic filter with a single chip CCD in conjunction with color wide dynamic range algorithms. It is also applicable, however, to other types of mosaic filters known in the art.

Description of the Prior Art

Various types of video enhancement apparatuses and techniques have been proposed. Prior implementations of color wide dynamic range cameras, such as those disclosed  
5 in the above-identified parent applications hereto, have used a plurality of CCD chips to generate the image data for subsequent processing. The use of multiple CCD chips, however, adds to the complexity and cost of the instrument. Moreover, current consumer video cameras, i.e., camcorders,  
10 almost universally use a single CCD chip. Therefore, a single CCD implementation is required to use dynamic range enhancement algorithms in a camcorder. Single CCD chip implementations are similarly preferred for endoscopic applications.

15

OBJECTS AND SUMMARY OF THE INVENTION

It is therefore an object of this invention to provide a color wide dynamic range camera implemented with a single CCD chip.

20

It is also an object of this invention to provide a color wide dynamic range camera which is adapted for use with a camcorder.

25

It is a further object of this invention to provide a color wide dynamic range camera which is adapted for use with a conventional endoscope.

These and other objects of the invention will be more apparent from the discussion below.

SUMMARY OF THE INVENTION

30

There is thus provided in accordance with the preferred embodiment of the present invention, video imaging apparatus including means for providing a plurality of video color images of a scene at different exposure levels using a single CCD chip, each color image being  
35 separated into several (e.g., four in the preferred

embodiment) different components prior to sensing by the CCD chip by way of a multiple color mosaic filter in front of the CCD chip. The pixel outputs are then decoded -- subjected to specific mathematical operations by the processing electronics following the CCD output -- to generate the video luminance and chrominance signals.

The present invention integrates the digital processing of the mosaic color CCD data with ADAPTIVE SENSITIVITY™ dynamic range enhancement. This integration provides for a substantial savings in total system processing hardware chip count and cost. It also permits better control of the color and detail production of the camera's video output. The mosaic storage format also provides for a unique video image compression technique.

#### BRIEF DESCRIPTION OF THE DRAWINGS

Further objects and advantages of the invention will become apparent from the following description and claims, and from the accompanying drawings, wherein:

Figure 1 is a general block diagram of the present invention.

Figure 2 is a representative illustration of the data image elements, with the size of the data image elements exaggerated.

Figure 3 is a general block diagram of the long and short processing of the present invention.

Figure 4 is a block diagram of the color path of the present invention.

Figure 5 is a block diagram of the intensity path of the present invention.

Figure 6 is a block diagram of the look-up table processing of the present invention.

Figure 7 is a block diagram of the joint operations of the present invention.

Figure 8 is a block diagram of the differential color, intensity result block of the present invention.

Figure 9 is a block diagram of the color suppression factor block of the present invention.

5 Figure 10 is a block diagram of the color conversion block of the present invention.

Figure 11 is a block diagram of the mosaic generation block of the present invention.

10 DETAILED DESCRIPTION OF THE PREFERRED EMBODIMENTS

Referring now to the drawings in detail wherein like numerals indicate like elements throughout the several views, one sees that Figure 1 is a block diagram of the apparatus 10 of the present invention.

15 Apparatus 10 includes a mosaic filter 12 which is bonded to the front of CCD 14 (preferably a single chip), generally as part of the CCD integrated circuit manufacturing process.

20 The alternating mosaic filter elements are cyan, magenta, yellow and green (wherein C 'cyan' = G 'green' + B 'blue'; M 'magenta' = R 'red' + B; and Ye 'yellow' = R+G). When the CCD 14 charge output is read out, the photoelectric charges from vertically adjacent sensor elements of CCD 14 are combined in the analog shift register (not shown). The on-chip addition gives rise to  $\alpha$ ,  $\beta$ ,  $\gamma$  and  $\delta$  elements as described below and as described in the Sony CCD 1992 Data Book (Sony part number ICX038AK), as well as earlier editions.

25 As shown in Figure 2, the mosaic complementary additive color image comprises alternating first and second rows of image data elements  $18_A - 18_D$ , wherein first rows include alternating  $\alpha$  and  $\gamma$  data elements ( $18_A$  and  $18_B$ , respectively), and wherein the second rows include alternating  $\beta$  and  $\delta$  data elements ( $18_C$  and  $18_D$ , respectively).  
35

The  $\alpha$  image data elements  $18_A$  are an equal mixture of cyan plus green (i.e.,  $C + G = B$  'blue' +  $2G$  'green'). The  $\gamma$  image data elements  $18_B$  are an equal mixture of magenta plus yellow (i.e.,  $M + Ye = 2R$  'red' +  $B + G$ ). Similarly, the  $\beta$  image data elements  $18_C$  are an equal mixture of cyan plus magenta (i.e.,  $C + M = 2B + G + R$ ) and the  $\delta$  image data elements  $18_D$  are an equal mixture of green plus yellow (i.e.,  $G + Ye = 2G + R$ ).

Those skilled in the art will recognize that:

$$Y \text{ (i.e., intensity)} = \frac{\alpha + \gamma}{2} = \frac{\beta + \delta}{2}$$

from which the definition of intensity (Y) in the red, green, blue (RGB) system may be derived:

$$Y = R + 1.5G + B$$

Of course, those skilled in the art will realize that other color combinations are equally applicable. Each mosaic element of filter 12 covers the sum of two adjacent pixel sensors of CCD 14 so that each pixel output of CCD 14 is representative of one of the above color combinations given for the various image data elements 18. Four different monochromatic images, each representative of one color combination chosen from the colors of image data elements  $18_A - 18_D$  of a given scene, are therefore generated by CCD 14.

As can be further seen from Figure 1, apparatus 10 includes four major functions as summarized below:

1. Long/short exposure processing:

The first stages of the algorithm are performed on the two exposures (long/short) separately. The processing of each exposure is divided into two paths:

- a. Color path processing - evaluates color component for each pixel.
- b. Intensity (Y) path processing - handles intensity information for each pixel. This includes point ("DC") intensity and edge information.

2. Point processing:

Each of the long/short exposure length processing functions (typically implemented on separate chips) outputs its point intensity information, obtained from the Y path processing, to four look-up tables (LUTs). These tables determine the point intensity result of the two exposures, the normalized color weighting or color selection function and the saturation color suppression factor. This information serves the joint operation processing stage. The four LUTs are programmable, thus enabling operation with different functions when necessary. In an alternative embodiment, these LUTs may be replaced by a programmable, piecewise linear (PWL) or other digital function generator.

3. Joint operations processing:

Joint operations processing joins results produced by the long and short processing blocks, and results obtained from the functions implemented in the table processing LUTs, and evaluates the final output of the algorithm. The processing is divided into:

- a. Color components and Y result calculation — evaluates the final result of the color components and the intensity of each pixel.
- b. Color suppression factor calculation — evaluates the color suppression factor for each pixel, based on both edges and saturation information.
- c. Color conversion processing — converts mosaic differential color space to RGB color space and produces RGB and Y/Cr/Cb outputs for each pixel.

4. Generate mosaic processing.

Generate Mosaic processing converts RGB color space back to mosaic color space for each pixel. The mosaic information generated enables economical hardware storage of processed images. This information can be retrieved and replayed through the algorithm — in

Replay Mode — to produce RGB or Y/Cr/Cb output of the stored result.

Referring now to Figure 1, similar to U.S. Patent No. 5,144,442 and parent U.S. patent application Serial No. 07/795,350 (the disclosures of which, again, along with U.S. patent application Serial No. 07/805,512 and U.S. Patent No. 4,858,014 are incorporated herein by reference), apparatus 10 includes long/short processing as implemented by mosaic long exposure field block 20 and mosaic short exposure field block 22 which obtain, respectively, a long and a short exposure from CCD 14 in order to allow subsequent processing by long exposure processing block 24 and short exposure processing block 26. The terms "long" and "short" exposures are used here generally to denote two image inputs to apparatus 10. In general, "long" is used to mean an input with a higher exposure level, and "short", a lower exposure level. The higher exposure may be generated in several ways, including longer integration time, typically obtained by controlling the "electronic shutter" of the CCD chip; higher gain in the analog amplifiers preceding digitization; or a larger mechanical iris opening or other external gating means.

These two image inputs are usually generated by a single CCD chip, but may also be generated simultaneously by two separate, boresighted CCD chips, as disclosed in the aforementioned earlier applications. For the more common case in which the two inputs are generated by a single CCD chip, they may be generated either sequentially (as in the case of the first method above — integration time control) or concurrently (by using two input channels with different gain levels). When a sequential method is used, field memories are required at the input to apparatus 10 (in blocks 20 and 22) to synchronize the data coming from the two sequential fields or frames. These memories are not needed in concurrent modes, except for purposes of

"freezing" the image for electronic, digital storage. Switching logic incorporated in blocks 20 and 22 controls the data flow into and out of these field memories, depending on which mode (sequential or concurrent) is used.

5 Of course, this implementation could be expanded to more than two exposure levels. Blocks 24 and 26 may typically be provided on separate processing chips or incorporated together in a single chip. The processing for each exposure is divided into two paths:

- 10 1. Color path processing — handles color information for each pixel (see color path block 28 in Figure 3 and, in more detail, in Figure 4); and
- 15 2. Intensity (Y) path processing — handles intensity information for each pixel (see Y path block 30 in Figure 3 and, in more detail, in Figure 5).

Additionally, as shown in more detail in Figure 3, long/short exposure processing blocks 24, 26 include mosaic white balance block 32.

20 Mosaic white balance block 32 receives the following field of information from long/short exposure field blocks 20, 22:

25

$\alpha$	$\gamma$	$\alpha$	$\gamma$	$\alpha$	$\gamma$	....
$\beta$	$\delta$	$\beta$	$\delta$	$\beta$	$\delta$	....
$\alpha$	$\gamma$	$\alpha$	$\gamma$	$\alpha$	$\gamma$	....
$\beta$	$\delta$	$\beta$	$\delta$	$\beta$	$\delta$	....
$\alpha$	$\gamma$	$\alpha$	$\gamma$	$\alpha$	$\gamma$	....
$\beta$	$\delta$	$\beta$	$\delta$	$\beta$	$\delta$	....
.	.	.	.	.	.	.
.	.	.	.	.	.	.
.	.	.	.	.	.	.

30

That is, the information from CCD 14 with the mosaic data order intact is received.

After processing, the mosaic white balance block 32 outputs color-corrected data values:

$\alpha_{wb} \gamma_{wb} \alpha_{wb} \gamma_{wb} \alpha_{wb} \gamma_{wb} \dots$   
 $\beta_{wb} \delta_{wb} \beta_{wb} \delta_{wb} \beta_{wb} \delta_{wb} \dots$   
 $\alpha_{wb} \gamma_{wb} \alpha_{wb} \gamma_{wb} \alpha_{wb} \gamma_{wb} \dots$   
 $\beta_{wb} \delta_{wb} \beta_{wb} \delta_{wb} \beta_{wb} \delta_{wb} \dots$   
5  $\alpha_{wb} \gamma_{wb} \alpha_{wb} \gamma_{wb} \alpha_{wb} \gamma_{wb} \dots$   
 $\beta_{wb} \delta_{wb} \beta_{wb} \delta_{wb} \beta_{wb} \delta_{wb} \dots$   
. . .  
. . .  
. . .

10 Mosaic white balance block 32 contains mosaic color  
balance functions. These functions may typically be  
implemented as eight mosaic white balance LUTs (look-up  
tables). That is, for each exposure there is a set of four  
LUTs, one for each mosaic data type:  $\alpha$ ,  $\beta$ ,  $\gamma$ , and  $\delta$ .  
15 Independent calculation of white balance correction factors  
is performed for each exposure. This enables white  
balancing scenes where the observable parts of the two  
exposures are at different color temperatures. The LUTs  
may contain multiplicative correction factors which are  
20 evaluated as follows:

From the definitions of  $\alpha$ ,  $\beta$ ,  $\gamma$ ,  $\delta$  and  $Y$  it follows,  
that for a white image (where by definition  $R=G=B$ ), the  
following relations should hold:

25  $\alpha_{wh} = \frac{6}{7} * Y$   
 $\beta_{wh} = \frac{8}{7} * Y$   
30  $\gamma_{wh} = \frac{8}{7} * Y$   
35  $\delta_{wh} = \frac{6}{7} * Y$

Based on these relations correction factors can be calculated by enforcing these relations on the average of a white image:

$$\begin{aligned}
 5 \quad C_\alpha &= \frac{\frac{6}{7} * \bar{Y}}{\bar{\alpha}} \\
 10 \quad C_\beta &= \frac{\frac{8}{7} * \bar{Y}}{\bar{\beta}} \\
 15 \quad C_\gamma &= \frac{\frac{8}{7} * \bar{Y}}{\bar{\gamma}} \\
 20 \quad C_\delta &= \frac{\frac{6}{7} * \bar{Y}}{\bar{\delta}}
 \end{aligned}$$

25 where  $\bar{Y}$  denotes a selective average over Y in the given white image and  $\bar{\alpha}$ ,  $\bar{\beta}$ ,  $\bar{\gamma}$  and  $\bar{\delta}$  are the respective average values of  $\alpha$ ,  $\beta$ ,  $\gamma$  and  $\delta$ . Saturated or cutoff pixels are excluded from this average. Since by definition,

$$30 \quad \bar{Y} = \frac{\bar{\alpha} + \bar{\gamma}}{2} = \frac{\bar{\beta} + \bar{\delta}}{2}$$

the equations for the correction factors are:

$$\begin{aligned}
 35 \quad C_\alpha &= \frac{3}{7} * \left( 1 + \frac{\bar{\gamma}}{\bar{\alpha}} \right) \\
 40 \quad C_\beta &= \frac{4}{7} * \left( 1 + \frac{\bar{\delta}}{\bar{\beta}} \right) \\
 45 \quad C_\gamma &= \frac{4}{7} * \left( 1 + \frac{\bar{\alpha}}{\bar{\gamma}} \right) \\
 50 \quad C_\delta &= \frac{3}{7} * \left( 1 + \frac{\bar{\beta}}{\bar{\delta}} \right)
 \end{aligned}$$

The LUT values are calculated by simple multiplication of each mosaic data type by its respective correction factor:

$$\begin{aligned} \alpha_{wb} &= \alpha * C_{\alpha} \\ \beta_{wb} &= \beta * C_{\beta} \\ \gamma_{wb} &= \gamma * C_{\gamma} \\ \delta_{wb} &= \delta * C_{\delta} \end{aligned}$$

5  
10  
15  
In an alternative embodiment, these LUTs are replaced by digital multipliers. Furthermore, the LUTs may also be loaded with correction functions other than simple linear multiplicative factors. Alternatively, the mosaic balance correction factors can be computed based on four average signals, namely,  $\alpha$ ,  $\beta$ ,  $\gamma$  and  $\delta$ , instead of merely two of them as above. This alternative yields improved uniformity of color balance under difficult conditions. Alternatively, the white balance function may be done on the RGB color components in the color conversion block 78 (described below).

20 Referring now to Figure 4, color path block 28 is shown in more detail. As previously stated, the input to color path block 28 is the image data  $\alpha_{wb}$ ,  $\beta_{wb}$ ,  $\gamma_{wb}$ ,  $\delta_{wb}$  after processing by mosaic white balance block 32.

25 The initial processing of color path block 28 is performed by color difference evaluation block 34 which receives data  $\alpha_{wb}$ ,  $\beta_{wb}$ ,  $\gamma_{wb}$ ,  $\delta_{wb}$  from mosaic white balance block 32 and calculates color difference components  $dr$ ,  $db$  for each pixel in the array:

$$\begin{aligned} dr \ dr \ dr \ . \ . \ . \ . &= (\gamma - \alpha) \ (\gamma - \alpha) \ (\gamma - \alpha) \ . \ . \ . \ . \\ db \ db \ db \ . \ . \ . \ . &= (\delta - \beta) \ (\delta - \beta) \ (\delta - \beta) \ . \ . \ . \ . \\ dr \ dr \ dr \ . \ . \ . \ . &= (\gamma - \alpha) \ (\gamma - \alpha) \ (\gamma - \alpha) \ . \ . \ . \ . \\ db \ db \ db \ . \ . \ . \ . &= (\delta - \beta) \ (\delta - \beta) \ (\delta - \beta) \ . \ . \ . \ . \end{aligned}$$

30 wherein:

$dr \equiv \gamma - \alpha$ , the differences between successive readings in even lines.

db =  $\delta - \beta$  , the differences between successive readings in odd lines.

The correct evaluation of dr and db requires horizontal interpolation as described in the following equations:

For each pixel (i,j) in even lines i:

$$dr(j_{\text{odd}}) = \gamma_{wb}(j_{\text{odd}}) - \frac{\alpha_{wb}(j_{\text{odd}}-1) + \alpha_{wb}(j_{\text{odd}}+1)}{2}$$

$$dr(j_{\text{even}}) = \frac{\gamma_{wb}(j_{\text{even}}-1) + \gamma_{wb}(j_{\text{even}}+1)}{2} - \alpha_{wb}(j_{\text{even}})$$

where j is the pixel index along the line (here and henceforth).

For each pixel (i,j) in odd lines i:

$$db(j_{\text{odd}}) = \delta_{wb}(j_{\text{odd}}) - \frac{\beta_{wb}(j_{\text{odd}}-1) + \beta_{wb}(j_{\text{odd}}+1)}{2}$$

$$db(j_{\text{even}}) = \frac{\delta_{wb}(j_{\text{even}}-1) + \delta_{wb}(j_{\text{even}}+1)}{2} - \beta_{wb}(j_{\text{even}})$$

Color difference components dr, db are thereafter received by low-pass color component block 36 which calculates a low-pass color component  $dr_{lp}$  or  $db_{lp}$  for each pixel:

$$dr_{lp} dr_{lp} dr_{lp} \dots = (\gamma - \alpha)_{lp} (\gamma - \alpha)_{lp} \dots$$

$$db_{lp} db_{lp} db_{lp} \dots = (\delta - \beta)_{lp} (\delta - \beta)_{lp} \dots$$

$$dr_{lp} dr_{lp} dr_{lp} \dots = (\gamma - \alpha)_{lp} (\gamma - \alpha)_{lp} \dots$$

$$db_{lp} db_{lp} db_{lp} \dots = (\delta - \beta)_{lp} (\delta - \beta)_{lp} \dots$$

Block 36 performs horizontal low-pass filtering on  $dr_{lp}$  and  $db_{lp}$  calculated in block 34. This reduces color artifacts caused by interpolation. In a preferred embodiment, the low-pass filter width is five pixels and its coefficients are  $\frac{1}{6}, \frac{1}{4}, \frac{1}{4}, \frac{1}{4}, \frac{1}{6}$ . The equations follow:

13

For pixels (i,j) in even lines i:

$$dr_p(j) = \frac{dr(j-2) + 2*dr(j-1) + 2*dr(j) + 2*dr(j+1) + dr(j+2)}{8}$$

For pixels (i,j) in odd lines i:

$$db_p(j) = \frac{db(j-2) + 2*db(j-1) + 2*db(j) + 2*db(j+1) + db(j+2)}{8}$$

Delay buffer 38 receives the output from low-pass color component block 36 and directs  $db_p(i_{even} - 1)$ ,  $dr_p(i_{odd} - 1)$ ,  $db_p(i_{even} + 1)$  and  $dr_p(i_{odd} + 1)$  to vertical interpolation block 40 and  $dr(i_{even})$  and  $db(i_{odd})$  to multiplexer 42.

Vertical interpolation block 40 receives the low-pass color components as described above and generates interpolated low-pass color components  $dr'_p$  in the odd numbered lines and  $db'_p$  in the even numbered lines:

$db'_p$   $db'_p$   $db'_p$   $db'_p$  . . . . .  
 $dr'_p$   $dr'_p$   $dr'_p$   $dr'_p$  . . . . .  
 $db'_p$   $db'_p$   $db'_p$   $db'_p$  . . . . .  
 $dr'_p$   $dr'_p$   $dr'_p$   $dr'_p$  . . . . .

The equations follow:

For even lines i:

$$db'_p(i, j) = \frac{db_p(i-1, j) + db_p(i+1, j)}{2}$$

For odd lines i:

$$dr'_p(i, j) = \frac{dr_p(i-1, j) + dr_p(i+1, j)}{2}$$

The interpolated low-pass color components  $dr_{lp}^i$ ,  $db_{lp}^i$  are multiplexed with the original low-pass components  $dr_{lp}$ ,  $db_{lp}$  to give the color path output values  $dr$  and  $dp$  for each pixel. This function is performed by multiplexer 42, which  
 5 separates the output received from delay buffer block 38 and vertical interpolator block 40 into a first path including  $db_{lp}^i(i_{even})$  and  $db_{lp}(i_{odd})$  and a second path including  $dr_{lp}(i_{even})$  and  $dr_{lp}^i(i_{odd})$ .

Referring now to Figure 5, which discloses in more  
 10 detail the intensity (Y) processing block 30 shown in Figure 3, one sees that the input to intensity (Y) processing block 30 from mosaic white balance block 32 (Figure 3) is received by intensity evaluation block 44 which outputs computed intensity Y for each pixel.

15 Since only one of the four data types ( $\alpha$ ,  $\beta$ ,  $\gamma$ ,  $\delta$ ) is present at any given pixel, the intensity evaluation block 44 calculation is performed as follows (based on the prior definition of Y):

For pixels (i,j) in even lines i:

$$20 \quad Y(j_{odd}) = \frac{\gamma(j) + \alpha(j-1)}{2}$$

$$25 \quad Y(j_{even}) = \frac{\alpha(j) + \gamma(j-1)}{2}$$

For pixels (i,j) in odd lines i:

$$30 \quad Y(j_{odd}) = \frac{\delta(j) + \beta(j-1)}{2}$$

$$Y(j_{even}) = \frac{\beta(j) + \delta(j-1)}{2}$$

The output from intensity evaluation block 44 is  
 35 received by delay buffer 46, generate output intensity block 48 and limit block 50.

Delay buffer 46 is a delay line of two horizontal lines, required for the 3x3 and 1x3 matrix transformations in Y path block 30. Together with the color path delay

buffer 38 and with Y path delay buffer 54, it may be implemented in a preferred embodiment in mosaic data space, operating on the input  $\alpha$ ,  $\beta$ ,  $\gamma$ ,  $\delta$  data before the intensity (Y) evaluation block 44 and color difference evaluation block 34. It is shown here schematically for clarity.

Vertical low-pass filter 52 receives intensity (Y) signals from the intensity evaluation block 44 as delayed by delay buffer 46. Block 52 generates the vertical low-pass intensity  $Y_{vlp}$  defined as:

$$Y_{vlp}(i,j) = \frac{Y(i-1,j) + 2Y(i,j) + Y(i+1,j)}{4}$$

The unfiltered intensity (Y) input will sometimes exhibit horizontal stripes, one pixel high in each field, in areas of transition to saturation. These stripes stem from the different color spectra of the  $\alpha$ ,  $\beta$ ,  $\gamma$ , and  $\delta$  pixels, as a result of which the  $\alpha+\gamma$  value of  $Y(i(\text{even}),j)$  may, for instance, reach saturation at a lower level of optical intensity than the  $\beta+\delta$  value of the vertically adjacent  $Y(i+1(\text{odd}),j)$ .  $Y_{vlp}$  averages these values to obtain a function that is smooth over the transition area.

Generate output intensity block 48 receives intensity (Y) information from intensity evaluation block 44 and vertical low-pass intensity ( $Y_{vlp}$ ) information from vertical low-pass filter 52. The output of block 48 is output intensity ( $Y_{out}$ ) to point processing LUT block 62 (see Figure 1).

Block 48 replaces the original luminance Y, computed by the intensity evaluation block 44, with  $Y_{vlp}$  when  $Y_{vlp}$  approaches saturation, in order to prevent the appearance of horizontal stripes as explained above. Block 48 implements the function:

16

$$Y_{out} = \begin{cases} Y & \text{if } Y_{vlp} < Y_{threshold} \\ Y_{vlp} & \text{if } Y_{vlp} \geq Y_{threshold} \end{cases}$$

The value of  $Y_{threshold}$  is typically equal to approximately  
 5 220 on an 8-bit scale of 0-255. As values of  $Y$  approach  
 saturation, image detail is lost in any event, so that  
 substituting  $Y_{vlp}$  in the high range does not adversely affect  
 the perceived resolution.  $Y_{vlp}$  is used as the selecting  
 input in order to ensure a smooth transition.

10 Limit block 50 receives intensity ( $Y$ ) signals from  
 intensity evaluation block 44 and generates limited  
 luminance  $Y_{limit}$ . Limit block 50 cuts off the upper range of  
 intensity ( $Y$ ) values that are to be input to edge detection  
 block 56, in order to prevent detection of false edges or  
 15 horizontal stripes that can arise in areas of transition to  
 saturation. Limit block 50 implements the function:

$$Y_{limit} = \min \{Y, Y_{lim}\}$$

the value of  $Y_{lim}$  is typically equal to approximately 220.

The output of limit block 50 (i.e.,  $Y_{limit}$ ) is delayed by  
 20 delay buffer 54 and received by edge detection block 56  
 which outputs edge information for each pixel.

Edge detector block 56 convolves the  $Y_{limit}$  value and its  
 8 immediate neighbors, with a high-pass or edge detecting  
 kernel.

25 In one embodiment, the 3x3 Laplacian operator may be  
 used:

$$30 \quad \frac{1}{8} * \begin{bmatrix} -1 & -1 & -1 \\ -1 & 8 & -1 \\ -1 & -1 & -1 \end{bmatrix}$$

Alternatively, to accommodate the geometric  
 characteristics of the CCD raster and to give greater

17

emphasis to the vertical edges, the following kernel may be used:

$$\frac{1}{8} * \begin{bmatrix} -\frac{1}{2} & -1 & -\frac{1}{2} \\ -2 & 8 & -2 \\ -\frac{1}{2} & -1 & -\frac{1}{2} \end{bmatrix}$$

In an alternative embodiment, the edge detector block 56 could be implemented as separate horizontal and vertical convolution operations (such as a 1 x 3 or 3 x 1 matrix), with additional logic to avoid overemphasis of diagonal edges. This alternative embodiment is less hardware intensive and gives improved picture quality in some circumstances.

Edge suppress block 58 receives the vertical low-pass intensity ( $Y_{vlp}$ ) signals from vertical low-pass filter 52 and outputs edge suppression function  $f_{edge}$  to edge multiplier 60.

The edge suppression function varies between 0 and 1 in the long exposure processing block 24 only. In the short exposure processing block 26, the function is set to 1, i.e., no edge suppression at this point. The function is typically implemented in block 24 in a piecewise linear fashion as follows:

$$f_{edge} = \begin{cases} 1 & \text{if } Y_{vlp} < \text{LOWSAT} \\ 1 - \frac{Y_{vlp} - \text{LOWSAT}}{\text{DEEPSAT} - \text{LOWSAT}} & \text{if } \text{LOWSAT} \leq Y_{vlp} < \text{DEEPSAT} \\ 0 & \text{if } \text{DEEPSAT} \leq Y_{vlp} \end{cases}$$

Typically LOWSAT is set to approximately 190 and DEEPSAT to approximately 220.

Edge multiplier 60 receives input from blocks 56, 58 and generates suppressed edge  $ed_{supp}$  to intensity (Y) result calculation.

Edge multiplier 60 multiplies the edge output of the edge detector block 56 by the edge suppression function  $f_{edge}$

from block 58 to generate an output value  $ed_{supp}$  to joint operations block 64 (see Figure 1). The purpose of this multiplication is to suppress distorted large edges that may appear in the long exposure at intensity (Y) values near saturation, at the same time as they appear in the short exposure at lower values of intensity (Y). The double appearance of such edges was found empirically to cause the resulting displayed edges to be overemphasized and sometimes smeared on account of blooming in the long exposure. The long exposure edge is suppressed so that only the short exposure edge will pass through to the output image. The edge suppress function may also be used to reduce the amplitude of edges from the long exposure which may be otherwise exaggerated due to the higher gain of the long exposure relative to the short exposure.

Additionally, as shown in phantom in Figure 5, an optional multiplier or LUT (block 57) may be added to multiply the output of block 56 times the ratio of exposure times (duration of long exposure/duration of short exposure) or the corresponding gain ratio, or some function of the exposure and/or gain ratio. This reflects the ratio of scales of these two values.

In the above manner, Y path block 30 outputs processed luminance  $Y_{out}$ , edge, and  $edge_{supp}$  to point processing block 62 and joint operations block 64.

Referring now to Figure 6, one sees that point processing block 62 includes four point processing functions, all of which receive output intensity ( $Y_{out}$ ) values from the long and short exposure processing blocks 24, 26 (see Figure 1). These functions may typically be implemented as LUTs in RAM or ROM memory. Point processing block 62 generates arbitrary function values for input to the joint operations block 64 (Figure 1).

The four tables of block 62 are:

1. The intensity (DC result) block 66 which generates a LUT value of intensity ( $Y_{lut}$ ) for the joint operations block 64.

5 Block 66 controls the amount of point ("DC") luminance that is summed with the edge information in generating the output luminance,  $Y_{result}$ . In its most general formulation,

$$10 \quad Y_{lut} = f(Y_{out}^{(short)}, Y_{out}^{(long)})$$

where  $f$  is an arbitrary function. It has been found that a quasilogarithmic or fractional power dependence of  $Y_{lut}$  on the inputs gives the best output image appearance, and the general function above can generally be reduced to a more compact LUT or piecewise linear implementation.

One simple possible computation of  $Y_{lut}$  is as follows:

- 20 a)  $Y_{short}$  is multiplied by the exposure ratio, so that it is on the same scale as  $Y_{long}$ . That is, if a certain pixel  $x$  is acquired within the active (linear) sensitivity region of both the short and long exposures, then  $Y_{long}(x) = R*Y_{short}(x)$ , where  $R$  is the exposure ratio,  $R = \text{long exposure time} / \text{short exposure time}$  (or any other ratio representing the two sensitivities).
- 25 b) Subsequently,  $Y_{long}$  and  $R*Y_{short}$  are linearly combined, so that the sum of their relative weights is always 1. That is,  $Y_{wdr} = a*Y_{long} + b*R*Y_{short}$ ,  $1 \geq a \geq 0$ ,  $1 \geq b \geq 0$ , and  $a+b=1$  (the wdr index stands for 'wide dynamic range'). The common practice is to set  $a=1$  in the region where the short exposure is cut-off (too dark),  $b=1$  in the region where the long exposure is saturated (too

bright), and  $a > 0$ ,  $b > 0$  in the region where both exposures carry meaningful information. However, this does not cover all cases, e.g. when neither exposure carries any information (long is saturated and short is cut-off, or both saturated, or both cut-off).

5

- c) Finally, the dynamic range of  $Y_{\text{wdr}}$  is reduced (yielding  $Y_{\text{lut}}$ ) by either a logarithmic function, or by multiplying it by a small fraction, or by using any empirically found mapping which resembles the log function or a similar contraction, e.g., the square root.

10

Other possible values for  $Y_{\text{lut}}$  comprise empirical modifications of the function described above.

15

2. & 3. Color weight normalize blocks 68, 70 for long and short exposures, respectively, which generate normalizing color weights  $w_l/Y_l$  and  $w_s/Y_s$ . Blocks 68 and 70 control the proportions of mixing the color values,  $dr$  and  $db$ , from the long and short exposures, respectively, that will be used to generate the output color values,  $dr_{\text{result}}$  and  $db_{\text{result}}$ . Generally,  $w_l$  and  $w_s$  are chosen so as to give predominant weight at each pixel to the color values taken from the exposure in which the intensity ( $Y$ ) luminance values are in the linear portion of the range, and to give a smooth transition over luminance gradient regions of the image. For the most part,  $w_l$  and  $w_s$  are determined on the basis of  $Y_{\text{out}}(\text{long})$  alone, except for cases where the long exposure is near saturation while the short is near cutoff, so that neither gives a linear reading.

20

25

30

35

The weighting values are complementary, i.e.,  $w_l = 1 - w_s$ , and  $w_l, w_s \geq 0$ . The outputs of blocks 68 and 70 are normalized by division by

5 the corresponding values of  $Y_{out}$  for the long and short exposures. Preferably, a floating point representation for the output values of blocks 68, 70 is used so as to maintain sufficient accuracy to prevent noticeable quantization in the output image.

10 Alternatively, instead of weighted addition of the normalized color from the two exposures, simple selection of the normalized color from one exposure or the other, with an ordered dither (alternation) of the color selection in areas of transition may be used. In this case, when  $w_l = 1$ , the color is selected from the long exposure; when  $w_s = 1$ , it is selected from the long exposure, and when neither  $w$  factor is 1, color values are taken alternately from long and short, according to a pseudo-random probability distribution in which the long and short color value probabilities are equal to the  $w_l$  and  $w_s$  values. A normalized color value that is an average of the long and short values may also be mixed into the dither, in order to give a smoother color transition.

4. 25 Saturation color suppression factor block 72 generates the color suppression factor  $W_{ht}$  that reduces chroma saturation (adds white to the image) in areas of luminance saturation of the input image. An additional edge color suppression factor,  $Z_{ed}$ , is computed in the joint operations block (as will be described hereinafter). The minimum of  $W_{ht}$  and  $Z_{ed}$ , both of which vary from 1 to 0, multiplies the chroma components at the output stage of color conversion. Thus, as  $W_{ht}$  approaches zero, so does the color saturation of the output image.

The purpose of the saturation color suppression function is to reduce the appearance of color artifacts that arise due to CCD saturation. The linear relationships between the  $\alpha$ ,  $\beta$ ,  $\gamma$ , and  $\delta$  CCD outputs and the true RGB colors break down as the CCD 14 approaches saturation. As non-linear deviations cannot be readily corrected, suspected distorted colors are "whitewashed". Similar techniques are used in the analog domain in conventional CCD cameras. As shown in Figure 6:

$$\text{Wht} = w_1 + w_2 * z_1$$

$w_1$  and  $w_2$  are identical to the above color weighting values. The variable  $Z_1$  is a function of  $Y_{\text{out}}(\text{short})$ , varying between 0 and 1, as shown schematically in the lower right corner of Figure 6. It tends to zero in areas where the short exposure luminance approaches either saturation or cutoff. This function will give  $\text{Wht} = 0$  at the saturation end (where generally  $w_2 = 1$  while  $w_1 = 0$ ). At the cutoff end, normally  $w_1 \approx 1$  as long as there is adequate overlap between the long and short exposures, so that in this range the function will usually give  $\text{Wht} \approx 1$ .

In normal mode, in which only one input channel is operative (see explanation below),  $\text{Wht} = 1$  from  $Y=0$  up to the low saturation threshold (typically 190). From this threshold up to the deep saturation limit of  $Y$  (typically 220),  $\text{Wht}$  drops linearly to its saturation value of 0. In replay mode (see below), there is no saturation color suppression.

Figure 7 discloses the joint operations block 64 (also see Figure 1).

Joint operations block 64 combines the chrominance and luminance data from the long and short exposure processing blocks 24, 26, together with data from point processing block 62, to generate a combined  $Y/dr/db$  result. Block 64 then converts this result to output in standard RGB or  $Y/Cr/Cb$  (luminance, chrominance (red) and chrominance (blue)) color space. A color suppression factor  $Z$  is computed and applied to the chrominance outputs in order to reduce color artifacts (by reducing chroma saturation) around edges and areas of luminance signal saturation.

Joint operations block 64 includes:

1. The  $dr$ ,  $db$ ,  $Y$  block 74 (recalling that  $dr$  and  $db$  are the differences between successive readings in even and odd lines, respectively) which receives  $dr$ ,  $db$  values from the color path outputs of long and short exposure processing blocks 24, 26 respectively;  $ed_{supp}$  from the intensity ( $Y$ ) path output of long exposure processing block 24 and edge data from the intensity ( $Y$ ) path output of short exposure processing block 26; and  $Y_{LUT}$ ,  $w_1/Y_1$  and  $w_2/Y_2$  from table processing (LUT) block 62. Block 74 generates combined intensity  $Y/dr/db$  results to color conversion block 78 (to be discussed). Block 74 will be discussed in greater detail hereinafter.
2. The color suppression factor block 76 which receives  $ed_{long}$  and  $ed_{short}$  from edge detector block 56 and saturation color suppression factor ( $Wht$ ) from point processing block 62 and generates chroma suppression factor  $Z$  for color conversion block 78. Block 76 will be discussed in greater detail hereinafter.

3. The color conversion block 78 which receives  $Y_{\text{result}}$ ,  $dr_{\text{result}}$ ,  $db_{\text{result}}$  from block 74 and  $Z$ , the color suppression factor from block 76 and generates  $R_{\text{out}}$ ,  $G_{\text{out}}$ , and  $B_{\text{out}}$  and  $Cr$  and  $Cb$ .  
5 Block 78 will be discussed in greater detail hereinafter.

The  $dr$ ,  $db$ ,  $Y$  block 74 is shown in further detail in Figure 8.

10 Block 74 includes an intensity ( $Y$ ) calculation which is performed by adders 79, 80 and edge limiting block 81. Adder 79 receives  $ed_{\text{supp}}$  (long) data from long exposure processing block 24, and  $ed_{\text{short}}$  from short exposure processing block 26. These two inputs are added to give  $edge_{\text{result}}$ , which is then input to the edge limiting block 81.  
15 Edge limiting is implemented as a piecewise linear function with 6 inflection points ( $A_1 \dots A_6$ ) and 4 slopes ( $S_1 \dots S_4$ ), as shown in the upper right inset of Figure 8. Generally the inflection points and slopes are chosen so as to enhance the smaller edges (i.e.,  $S_2$  and  $S_3 \geq 1$ ), while large edges (edge  $> A_5$  or  $< A_2$ ) are suppressed. Since these large edges  
20 come through strongly in the  $Y_{\text{LUT}}$  contribution anyway, the output image has a more pleasing appearance if they are not additionally enhanced.  $A_3$  and  $A_4$  may be set to 0, but it is sometimes desirable to set them to small non-zero values in  
25 order to suppress false edges due to noise. The best results appear to be obtained with  $|A_1|$  and  $|A_6|$  values of 50 to 60. The best values of the slopes  $|S_i|$  are typically in the range 0.5 to 2, but the hardware allows a greater range.

30 The  $edge_{\text{limited}}$  output is then summed by adder 80 with the  $Y_{\text{LUT}}$  output of block 62 to obtain the output luminance value  $Y_{\text{result}}$ . Additionally, as shown in phantom in Figure 10, adder 80 may be removed from its location in Figure 8 and placed

so that the output of block 81 is not added to  $Y_{result}$  until just before being added into block 113<sub>A-C</sub>, that is, as late as possible.

5           Block 74 further includes a  $dr$ ,  $db$  calculation which is performed by the remaining sections of block 74. The  $dr$ ,  $db$  calculation receives low-pass color components  $dr$ ,  $db$  from the color paths of long and short exposure processing blocks 24, 26;  $w_l/Y_l$  and  $w_s/Y_s$  from block 62; and  
10  $Y_{result}$  as calculated by adder 80. The  $dr$ ,  $db$  calculation outputs  $dr_{result}$  and  $db_{result}$ .

The long and short values of  $dr$  and  $db$  are multiplied by the respective normalized color weights,  $w_l/Y_l$  and  $w_s/Y_s$ , by multipliers 82, 84, 86, 88. These normalized, weighted  
15 color values from the two exposures are summed together by adders 90, 92 and then multiplied by  $Y_{result}$  by multipliers 94, 96 to give the scaled values:

$$20 \quad \begin{aligned} dr_{result} &= Y_{result} * \left\{ dr_l \frac{w_l}{Y_l} + dr_s \frac{w_s}{Y_s} \right\} \\ db_{result} &= Y_{result} * \left\{ db_l \frac{w_l}{Y_l} + db_s \frac{w_s}{Y_s} \right\} \end{aligned}$$

Alternatively,  $dr_{result}$  and  $db_{result}$  may be generated by  
25 selection between the long and short normalized  $dr$  and  $db$  inputs (and possibly their long/short average values).

The color suppression factor block 76 of Figure 7 is shown in more detail in Figure 9.

Maximum value block 100 selects the higher of the two  
30 absolute values of  $ed_{long}$  and  $ed_{short}$  as calculated by absolute value blocks 98, 99. The result of the calculation of block 100,  $ed_{max}$ , is input to edge chroma suppression factor block 102 to calculate  $Z_{cd}$ . The calculation of  $Z_{cd}$  is implemented as a piecewise linear function, shown in the  
35 upper right corner of Figure 9. As can be seen in Figure 9,  $Z_{cd}$  receives a value between  $Th$  and 1, given by:

$$Z_{cd} = \begin{cases} 1 & \text{if } ed_{\max} < E1 \\ Th + \frac{E2 - ed_{\max}}{E2 - E1} (1 - Th) & \text{if } E1 \leq ed_{\max} < E2 \\ Th & \text{if } E2 \leq ed_{\max} \end{cases}$$

Typically,  $E1=10$  and  $E2=27$  have been found to give good results. The minimum value of  $Z_{cd}$ ,  $Th$ , is ordinarily set to zero, to give complete chroma suppression at very strong edges.  $Th \neq 0$  is used only in replay of images stored in mosaic format (see generate mosaic block 120 described hereinafter), in which case  $Z_{cd}$  serves to suppress color anomalies resulting from the reinterpolation of the pixel values.

Thereafter, as shown in Figure 9, minimum value block 104 selects the minimum of the two color suppression factors,  $Z_{cd}$  and  $Wht$ , thereby determining the edge criterion or saturation criterion that should be used to provide the required degree of chroma suppression at the given pixel.

Referring now to Figure 10, which discloses in detail color conversion block 78 of Figure 7, one sees that color conversion block 78 receives  $Y_{\text{result}}$ ,  $dr_{\text{result}}$ , and  $db_{\text{result}}$  from block 74 and  $Z$  from block 76 and generates outputs in both the RGB and Y/Cr/Cb formulations.

In other words, block 78 takes the interim dynamic range enhancement results  $Y/dr/db$ , and converts them into conventional color components for system output.

Block 78 includes horizontal low-pass filter 106 which receives  $Y_{\text{result}}$  and calculates  $Y_{\text{result}}(lp)$  for the color matrix block 108.

Horizontal low-pass filter 106 is identical to the low-pass color component block 36 in the color path block 28 (see Figures 3 and 4). Since the  $dr$  and  $db$  inputs to the color matrix 108 have already been low-pass filtered by this low-pass filter operator, it is necessary to filter

the intensity (Y) value as well in order to prevent color artifacts.

Color matrix block 108 receives  $Y_{\text{result}}$  (lp) from horizontal low-pass filter 106 and  $dr_{\text{result}}$  and  $db_{\text{result}}$  from block 74 and generates low-pass RGB color component outputs.

If one recalls the derivation of Y, dr and db from the original  $\alpha$ ,  $\beta$ ,  $\gamma$  and  $\delta$  values of the mosaic CCD input:

$$\begin{aligned}
 Y &\equiv \frac{\alpha + \gamma}{2} \equiv \frac{\beta + \delta}{2} \\
 dr &\equiv \gamma - \alpha \\
 db &\equiv \delta - \beta
 \end{aligned}$$

together with the RGB equivalencies of  $\alpha$ ,  $\beta$ ,  $\gamma$  and  $\delta$ , one obtains the following relationships between RGB and the Y/dr/db values:

$$\begin{bmatrix} R \\ G \\ B \end{bmatrix} = 3.5 * \begin{bmatrix} 0.2 & 0.4 & 0.1 \\ 0.4 & -0.2 & 0.2 \\ 0.2 & -0.1 & -0.4 \end{bmatrix} \begin{bmatrix} Y \\ dr \\ db \end{bmatrix}$$

The factor of 3.5 is required for normalization of the relation  $Y = R + 1.5G + B$ . Due to hardware implementation considerations, the color conversion matrix is calculated as follows:

$$\begin{bmatrix} R \\ G \\ B \end{bmatrix} = 0.7 * \begin{bmatrix} 1.0 & 2.0 & 0.5 \\ 2.0 & -1.0 & 1.0 \\ 1.0 & -0.5 & -2.0 \end{bmatrix} \begin{bmatrix} Y \\ dr \\ db \end{bmatrix}$$

In this way the matrix multiplication is performed by a series of shift/add operations. The multiplicative factor 0.7 is combined (by multiplication) with externally programmed RGB white balance correction factors as is described hereinafter.

RGB white balance multipliers  $109_A$ ,  $109_B$ ,  $109_C$  receive low-pass RGB signals from color matrix block 108 and generate normalized low-pass RGB signals.

Multipliers  $109_A$ ,  $109_B$ ,  $109_C$  multiply each of the RGB low-pass values by a pre-computed white balance correction factor, adjusted by the normalization factor 0.7 required by the color matrix calculation. Although conventional RGB white balancing uses only two multiplicative factors, correcting R and B while G is held constant, this "short cut" does not preserve constant Y achromatic luminance. This loss of normalization may lead to the appearance of artifacts and incorrect luminance in the output. It is necessary, therefore, to use three multiplicative factors, normalized to preserve constant luminance Y.

The calculation of the correction factors is performed off-line by capturing a white image and selectively computing average values  $\bar{R}$ ,  $\bar{G}$ ,  $\bar{B}$ , and  $\bar{Y}$ , excluding pixels near saturation or cutoff. From the definition  $Y = R + 1.5G + B$ , it follows that for a corrected pixel in the white image, it should be found that:

$$R = G = B = \frac{1}{3.5} Y$$

From this relationship one derives the correction factors to be used in multipliers  $109_A$ ,  $109_B$ ,  $109_C$ :

$$R \text{ factor} = \frac{1}{3.5} \frac{\bar{Y}}{\bar{R}}$$

$$G \text{ factor} = \frac{1}{3.5} \frac{\bar{Y}}{\bar{G}}$$

$$B \text{ factor} = \frac{1}{3.5} \frac{\bar{Y}}{\bar{B}}$$

Output signal enhancement block 110 (which includes chroma suppression and RGB output functions) receives

corrected low-pass RGB color component signals from color matrix block 108 via multipliers  $109_A$ ,  $109_B$ ,  $109_C$ ;  $Y_{result}$  from block 74;  $Y_{result}$  (lp) from block 106; and chroma suppression factor Z from block 76.

5 As noted above, the RGB values output from color matrix block 108 are low-pass values. High-frequency image information is "re-injected" into RGB according to the following equation (given here only for the R component, since the treatment of G and B is identical):

$$10 \quad R_{lp} = R_{lp} + K * Y_{result} - K * Y_{result}^{(lp)}$$

K is an arbitrary constant between 0 and 1, chosen according to the degree of high-frequency enhancement required. Values in the range  $0.4 \leq K \leq 0.8$  are typically used.

15 The addition and subtraction of  $Y_{result}$  values to the RGB components can alter the original values of R/G and B/G, with the result that the correct hue of the image is not preserved. Therefore, in an alternative embodiment, R, G and B are multiplied by a high-pass enhancement function.

20 Since the RGB color component values contain both luminance and chrominance information, the chroma suppression factor, Z, is best applied to chrominance-only components, by adders  $113_A$ ,  $113_B$ ,  $113_C$ :

$$25 \quad Cr = R - Y_{result}$$

$$Cg = G - Y_{result}$$

$$Cb = B - Y_{result}$$

30 Combining these equations with the previous ones for "high frequency re-injection", one obtains the following formula, which is implemented as shown in Figure 10 (including arithmetic element blocks 114, 115, 116) to obtain Cr from  $R_{lp}$ :

$$Cr = R_{ip} + K*(Y_{result} - Y_{result}^{(lp)}) - Y_{result}$$

and likewise for Cg and Cb. These Cr/Cg/Cb values are multiplied by Z by multipliers 112<sub>A</sub>, 112<sub>B</sub>, 112<sub>C</sub>. At this point, Y/Cr/Cb output is available directly (using Y = Y<sub>result</sub>), though it is preferable to add a bias of +128 to the signed digital outputs Cr and Cb in order to convert them to positive values for D/A conversion. In the alternative, Y<sub>result</sub> can be added back into the chroma-suppressed Cr/Cg/Cb values (by adders 113<sub>A</sub>-113<sub>C</sub>) to obtain the final R<sub>out</sub>/G<sub>out</sub>/B<sub>out</sub>.

Referring now to Figure 11, which discloses generate mosaic block 120 of Figure 1 in more detail, one sees that the input of generate mosaic block 120 is R<sub>out</sub>/G<sub>out</sub>/B<sub>out</sub> from color conversion block 78 of joint operations block 64. The output of block 120 is the equivalent  $\alpha$ ,  $\beta$ ,  $\gamma$ ,  $\delta$  values in the format:

$$\begin{matrix} \alpha_{eq} & \gamma_{eq} & \alpha_{eq} & \gamma_{eq} & \cdot & \cdot & \cdot & \cdot & \cdot & \cdot \\ \beta_{eq} & \delta_{eq} & \beta_{eq} & \delta_{eq} & \cdot & \cdot & \cdot & \cdot & \cdot & \cdot \\ \alpha_{eq} & \gamma_{eq} & \alpha_{eq} & \gamma_{eq} & \cdot & \cdot & \cdot & \cdot & \cdot & \cdot \\ \beta_{eq} & \delta_{eq} & \beta_{eq} & \delta_{eq} & \cdot & \cdot & \cdot & \cdot & \cdot & \cdot \end{matrix}$$

In order to reduce memory requirements for image storage and to allow stored images to be replayed through the apparatus 10 for display, the final RGB values from the processed image are used to generate equivalent, simulated mosaic values of  $\alpha$ ,  $\beta$ ,  $\gamma$ , and  $\delta$ . In this way, only eight bits per pixel of information must be stored, rather than the 24 bits of full output information. These mosaic values can later be replayed to regenerate the stored image.

The simulated mosaic values are generated by the following matrix in matrix block 122, based on the color equivalencies given hereinabove.

$$\begin{matrix} 5 \\ \\ \\ \end{matrix}
 \begin{pmatrix} \alpha_{eq} \\ \beta_{eq} \\ \gamma_{eq} \\ \delta_{eq} \end{pmatrix}
 = \frac{1}{4} *
 \begin{pmatrix} 0 & 2 & 1 \\ 1 & 1 & 2 \\ 2 & 1 & 1 \\ 1 & 2 & 0 \end{pmatrix}
 \begin{pmatrix} R \\ G \\ B \end{pmatrix}$$

10           The factor of  $\frac{1}{4}$  that multiplies the matrix is used for reasons of hardware convenience — in order to ensure that  $\alpha$ ,  $\beta$ ,  $\gamma$ , and  $\delta$  do not overflow the range 0-255 of 8 bits. To maintain the normalization relations given hereinabove, the factor should actually be 1/3.5. Therefore, in replay mode, mosaic white balance block 32 is used to multiply the  $\alpha$ ,  $\beta$ ,  $\gamma$ , and  $\delta$  values back by 4/3.5 (=8/7) before reprocessing. Finally, multiplexer 124 selects which one of the four mosaic values to output for each pixel according to the table:

20

		j even	j odd
	i even	$\alpha$	$\gamma$
	i odd	$\beta$	$\delta$

25

Apparatus 10 has three modes of operation: normal, adaptive sensitivity (AS), and replay.

30   1. Normal mode emulates the performance of a mosaic color CCD camera without adaptive sensitivity. In this mode only the long exposure portion of the pipeline operates. The processing functions are limited to decoding the mosaic input into conventional color components: Y/Cr/Cb or RGB, while additionally performing filtering operations for anti-aliasing, detail (edge) enhancement and chroma suppression where required.

35

2. Adaptive sensitivity mode uses all the resources of the processing pipeline to generate wide dynamic range images as described hereinabove.

5 3. Replay mode is required for displaying images that have been stored in RAM or disk. Apparatus 10 stores these images in a regenerated mosaic format in order to save on storage memory requirements. Replay mode is similar to normal mode, except that most of the enhancement operations are not performed: since the stored data have already been  
10 filtered once, it is for the most part not desirable to filter them again.

The preceding specific embodiments are illustrative of the practice of the invention. It is to be understood, however, that other expedients known to those skilled in  
15 the art or disclosed herein, may be employed without departing from the spirit of the invention or the scope of the appended claims.

CLAIMSWhat is Claimed is:

1. A color wide dynamic range video imaging apparatus comprising:

5        sensor means for providing a plurality of color video images of a scene at different exposure levels;

      means for dividing each color video image into components; and

      means for processing said components of each of said  
10 plurality of video images to produce a combined color video image including image information from said components of each of said plurality of color video images by applying neighborhood transforms to at least one of said components of each of said plurality of video images,

15        wherein said means for processing includes means for calculating point intensity data for said each of said plurality of said video images.

2. The color wide dynamic range video imaging  
20 apparatus of Claim 1, wherein said means for processing includes means for calculating color weighting factors.

3. The color wide dynamic range video imaging  
25 apparatus of Claim 2, wherein said means for processing includes means for calculating saturation color suppression factors.

4. The color wide dynamic range video imaging  
30 apparatus of Claim 1, wherein said means for dividing each color video image into components includes a filter means in front of said sensor means and said filter means includes filter elements of a plurality of colors, said plurality of colors corresponding to said components.

5. The color wide dynamic range video imaging apparatus of Claim 4, wherein said sensor means includes a plurality of pixel sensing elements and

5 wherein said filter elements are arranged in a regular repeating pattern with each filter element in front of a single pixel element of said sensing means.

6. The color wide dynamic range video imaging apparatus of Claim 5, wherein said processing means  
10 includes means for evaluating an intensity of each color component;

means for evaluating color suppression factors for each pixel; and

15 means for converting said components into RGB color space.

7. The color wide dynamic range video imaging apparatus of Claim 6, wherein said means for evaluating an intensity of each color component communicates with a means  
20 for substituting luminance values when luminance otherwise approaches saturation.

8. The color wide dynamic range video imaging apparatus of Claim 6, wherein said means for evaluating an intensity of each color component communicates with a means  
25 for limiting luminance values.

9. The color wide dynamic range video imaging apparatus of Claim 5, wherein said processing means  
30 includes white balancing means which calculates correction factors for said components based upon the intensity of said color video images.

10. The color wide dynamic range video imaging apparatus of Claim 9, wherein white balancing means  
35

calculates an average intensity of said color video images excluding saturated pixels and cut-off pixels.

5           11. The color wide dynamic range video imaging apparatus of Claim 9, including vertical low-pass filter means receiving intensity and false edge suppression means, wherein said false edge suppression means receives intensity data from said vertical low-pass filter means and calculates false edge suppression factors which are reduced  
10 when said intensity data exceeds a pre-selected saturation value.

15           12. The color wide dynamic range video imaging apparatus of Claim 11, wherein said false edge suppression means calculates said false edge suppression factors for an image of a longest of said different exposure levels.

20           13. The color wide dynamic range video imaging apparatus of Claim 12, further including edge detection means and wherein an output of said edge detection means is multiplied times said false edge suppression factors.

25           14. The color wide dynamic range video imaging apparatus of Claim 5, wherein color components are calculated by multiplying an intensity times a sum of products of prior color components and output of said means for calculating said color weighting factors.

30           15. The color wide dynamic range video imaging apparatus of Claim 6, including means for calculating white balance correction factors for said components converted into RGB color space, wherein said white balance correction factors for a given respective RGB component are calculated by dividing average overall luminance by a multiple of an  
35 average value of said respective given RGB component.

16. The color wide dynamic range video imaging apparatus of Claim 15, wherein said average value of said respective given RGB component is calculated excluding pixels which are substantially near saturation or substantially near cut-off.

17. The color wide dynamic range video imaging apparatus of Claim 6, including means for converting said RGB color space components into mosaic color components corresponding to colors of said filter elements of said filter means.

18. The color wide dynamic range video imaging apparatus of Claim 1, wherein said means for processing is implemented on a single chip.

19. An imaging apparatus comprising:  
sensor means for providing a plurality of color video images of a scene at different exposure levels;  
means for dividing each color video image into components; and  
means for processing said components of each of said plurality of video images to produce a combined color video image including image information from said components of each of said plurality of color video images by applying neighborhood transforms to at least one of said components of each of said plurality of video images,  
wherein said means for processing includes means for calculating point intensity data for said each of said plurality of said video images, and  
wherein said processing means includes white balancing means which calculates correction factors for said components based upon the intensity of said color video images.

35

20. A color wide dynamic range video processing chip comprising:

5 means for processing components of each of a plurality of video images of a scene at different exposure levels to produce a combined color video image including image information from said components of each of said plurality of color video images by applying neighborhood transforms to at least one of said components of each of said plurality of video images,

10 wherein said means for processing includes means for calculating point intensity data for said each of said plurality of said video images.

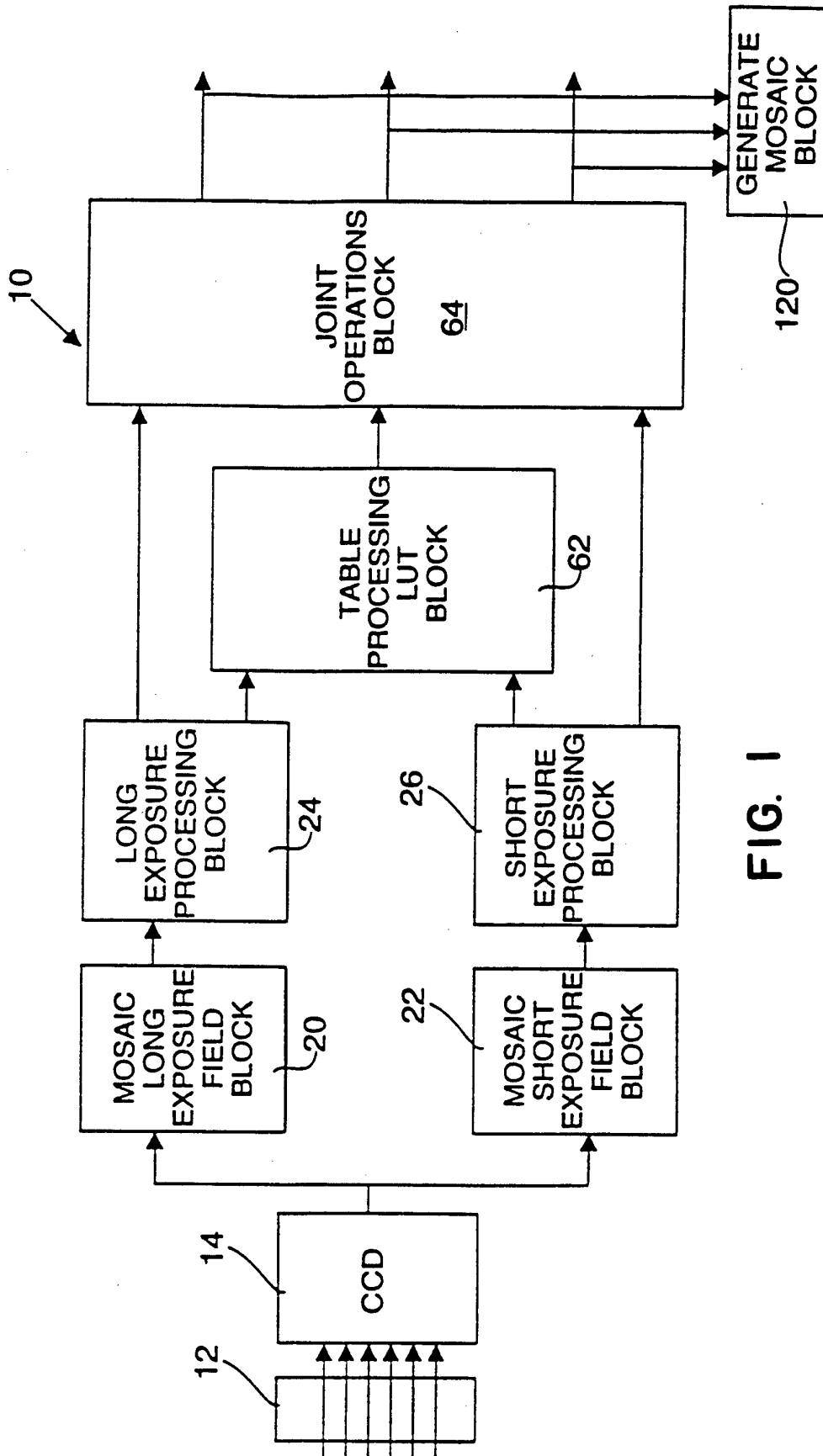


FIG. 1

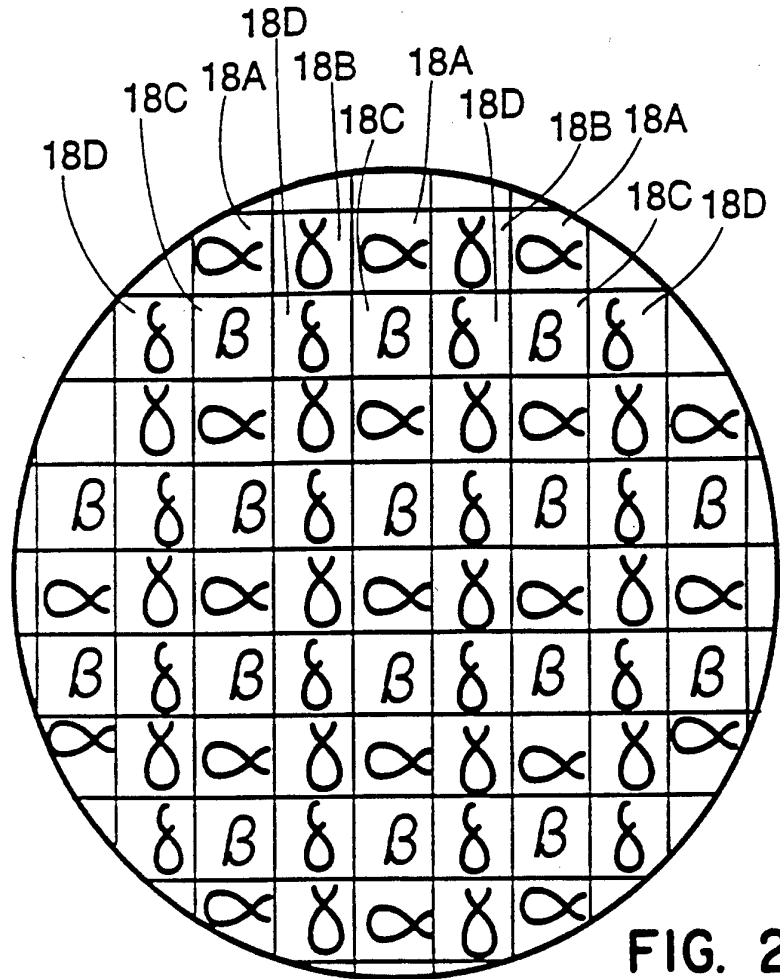


FIG. 2

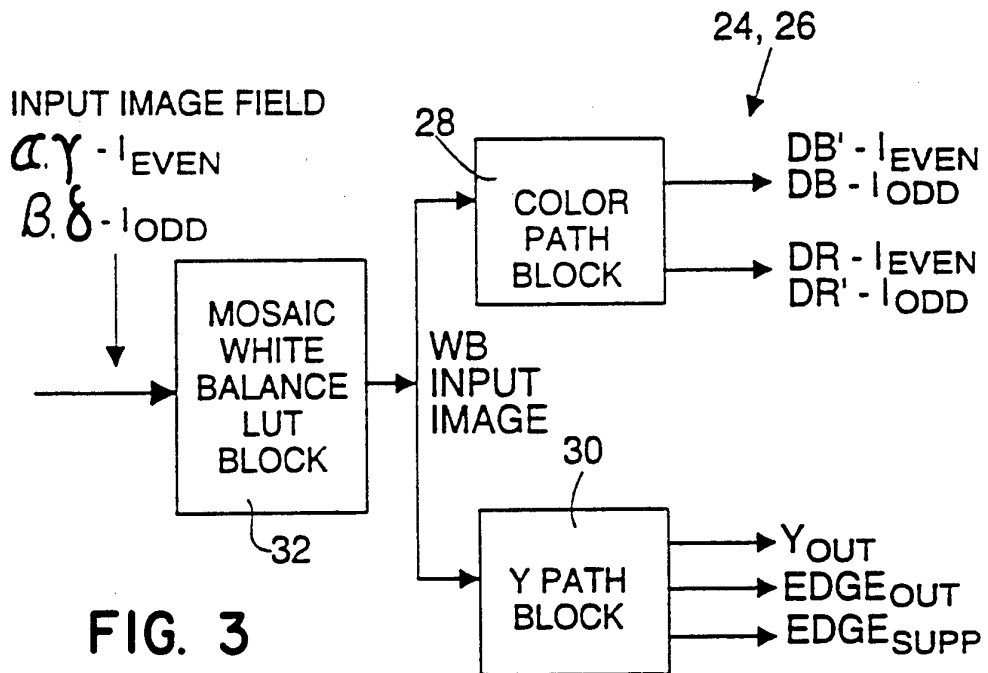


FIG. 3

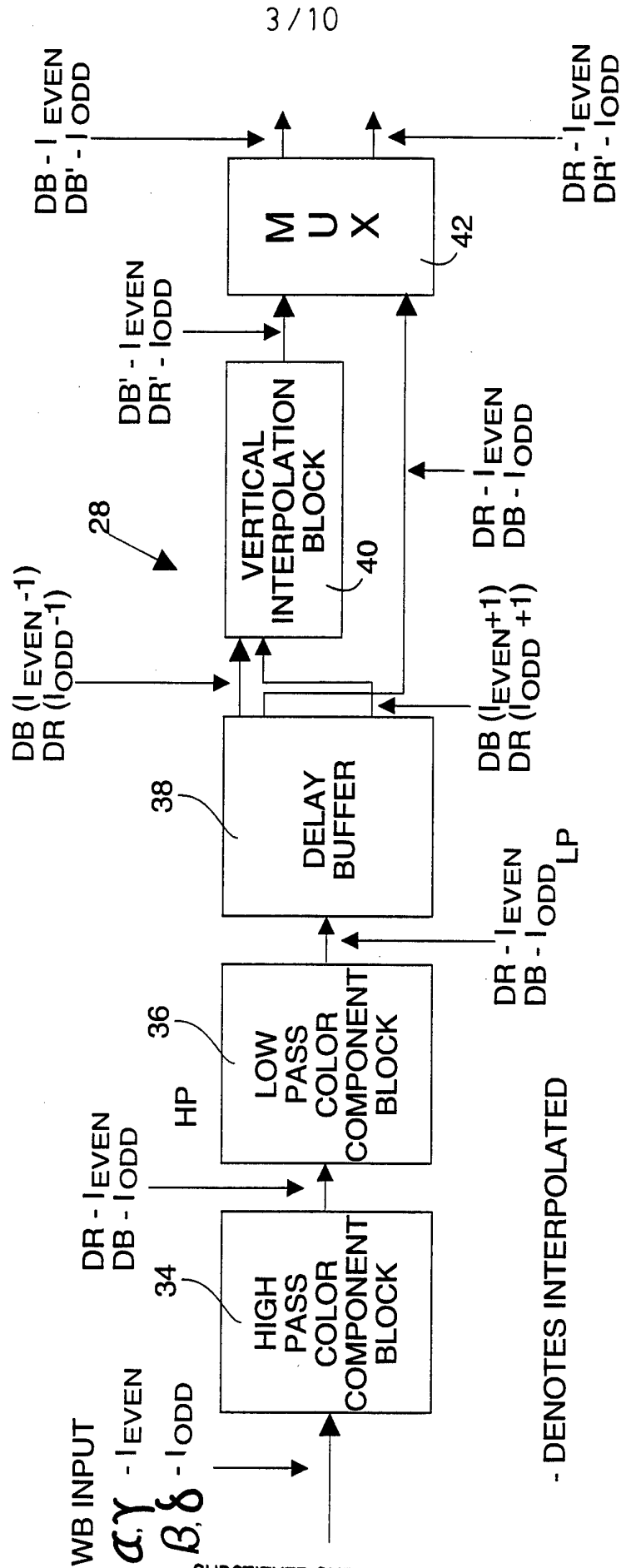


FIG. 4

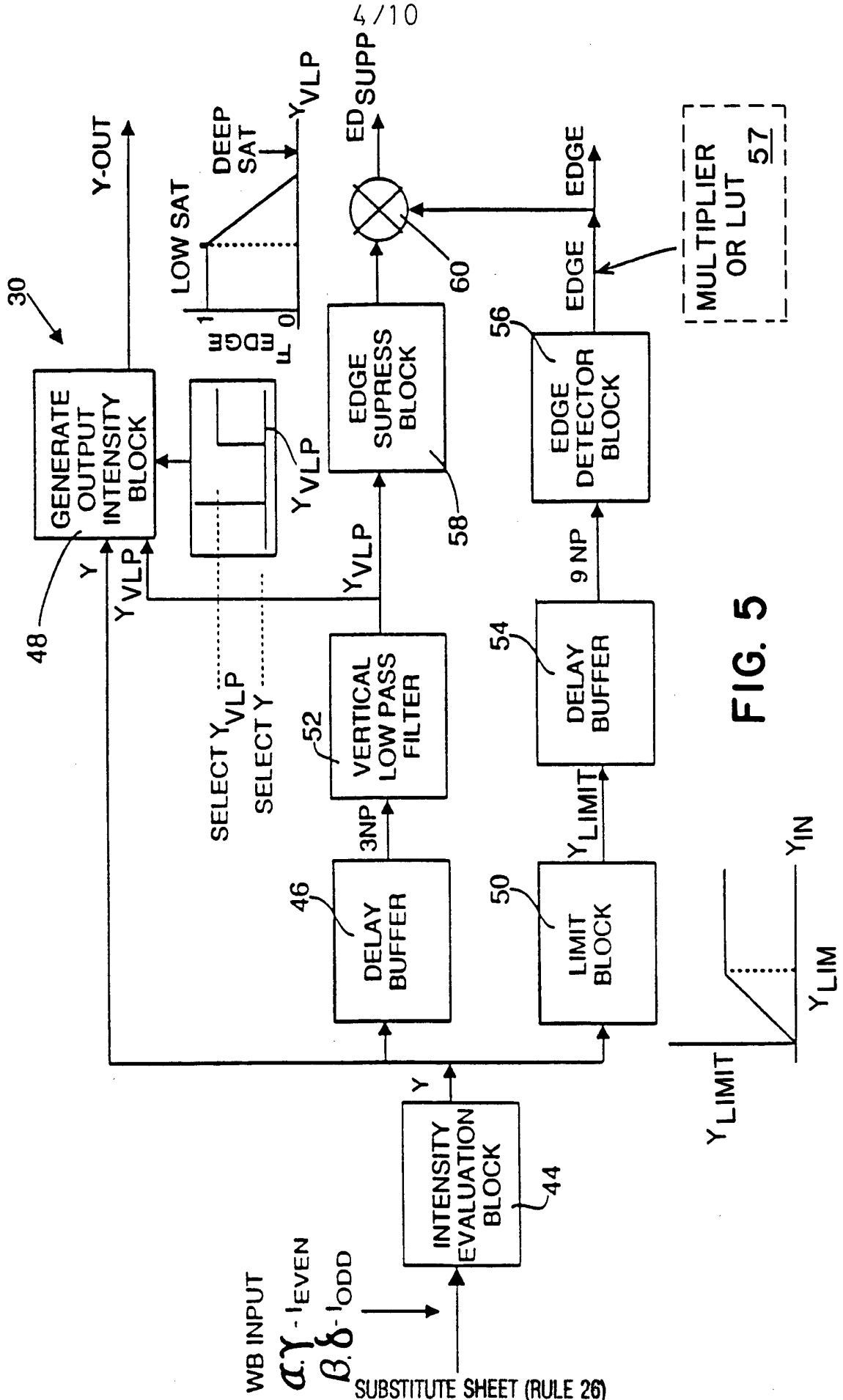


FIG. 5

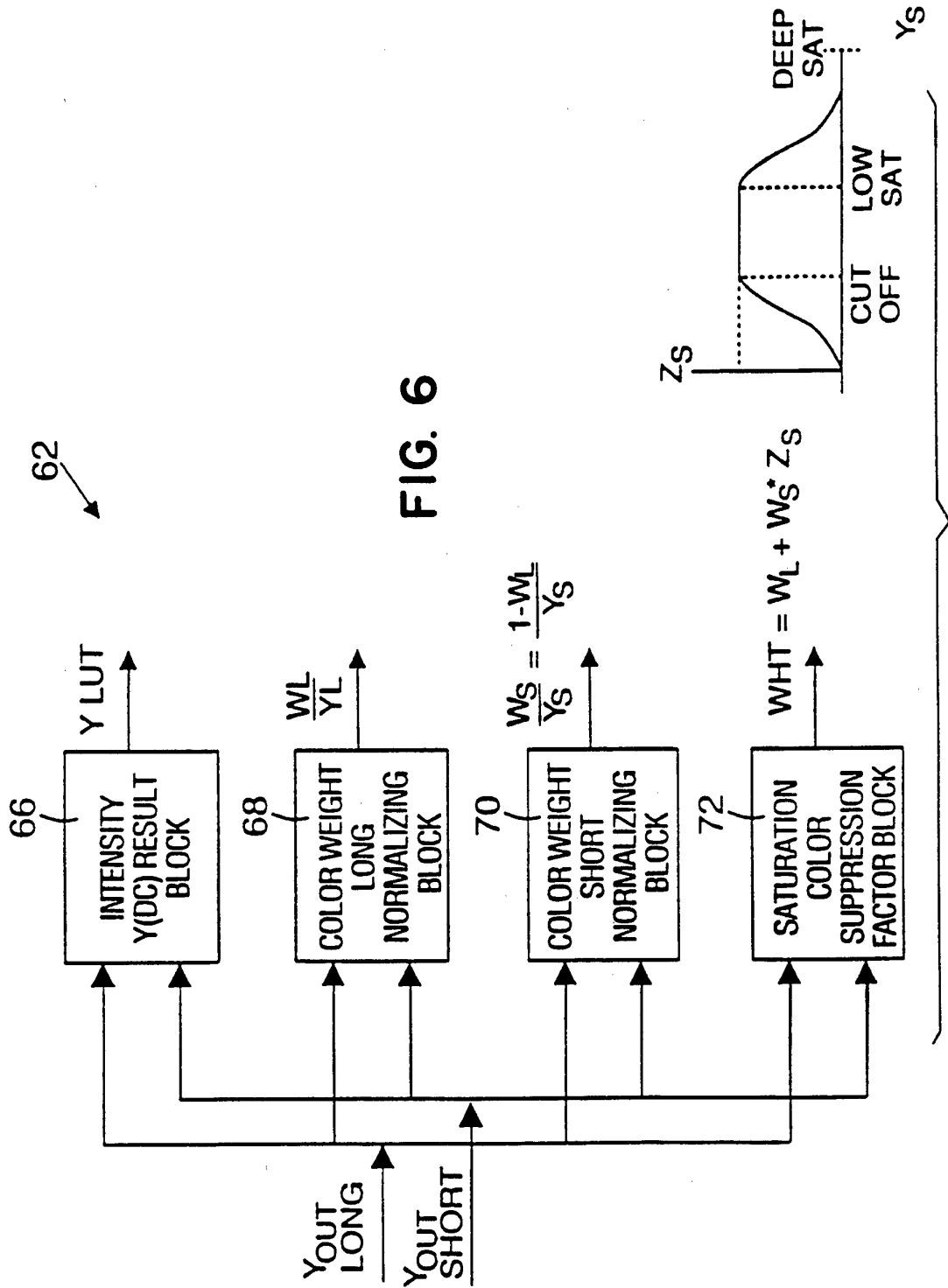


FIG. 6

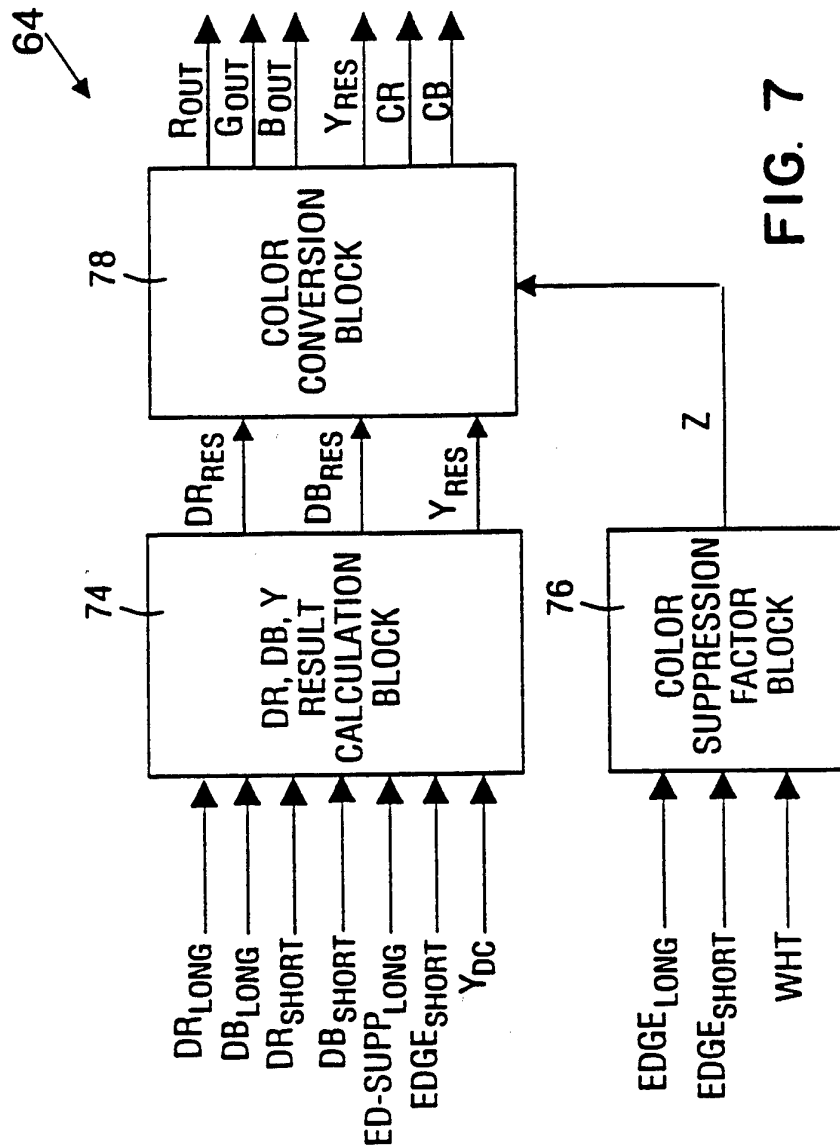


FIG. 7

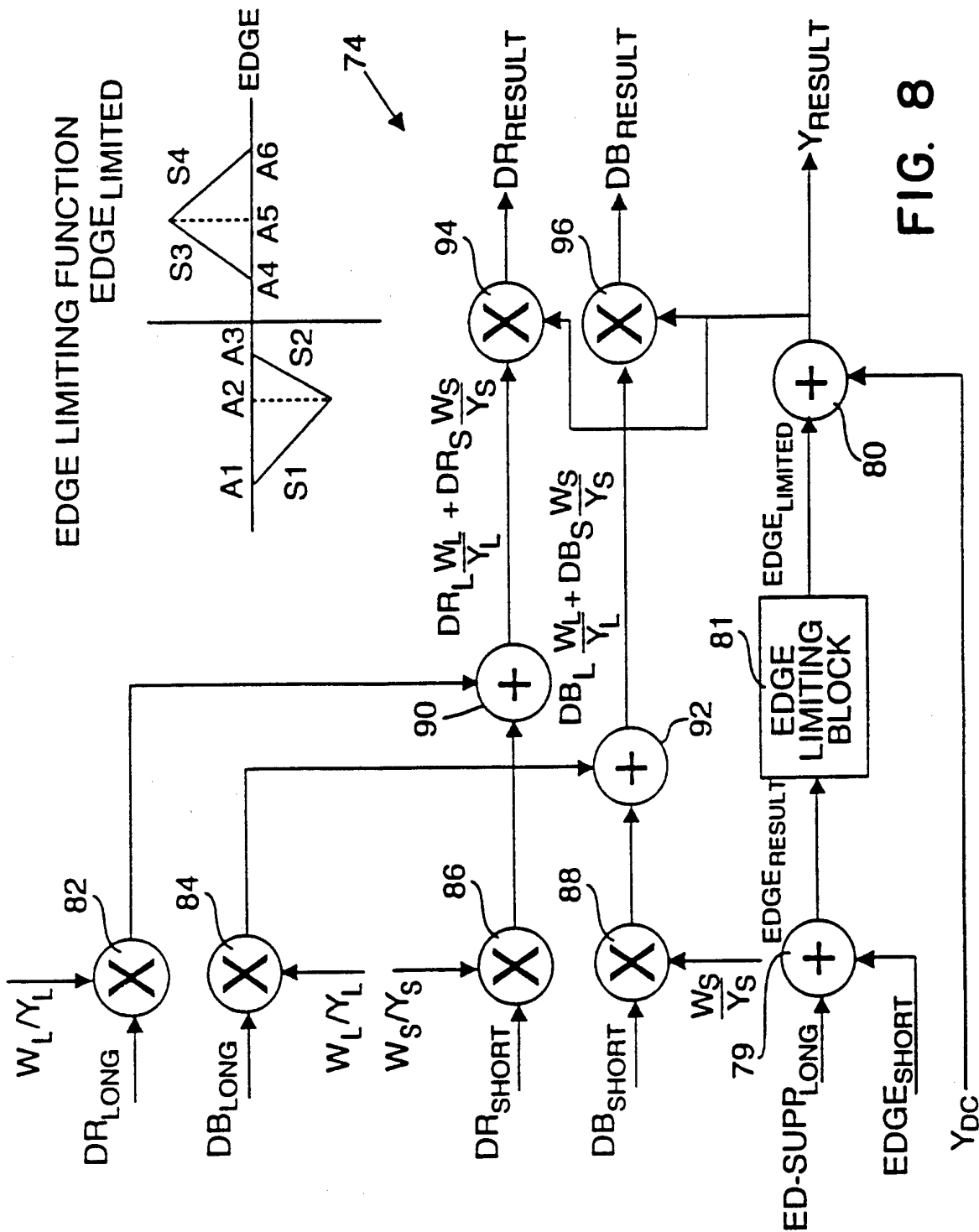


FIG. 8

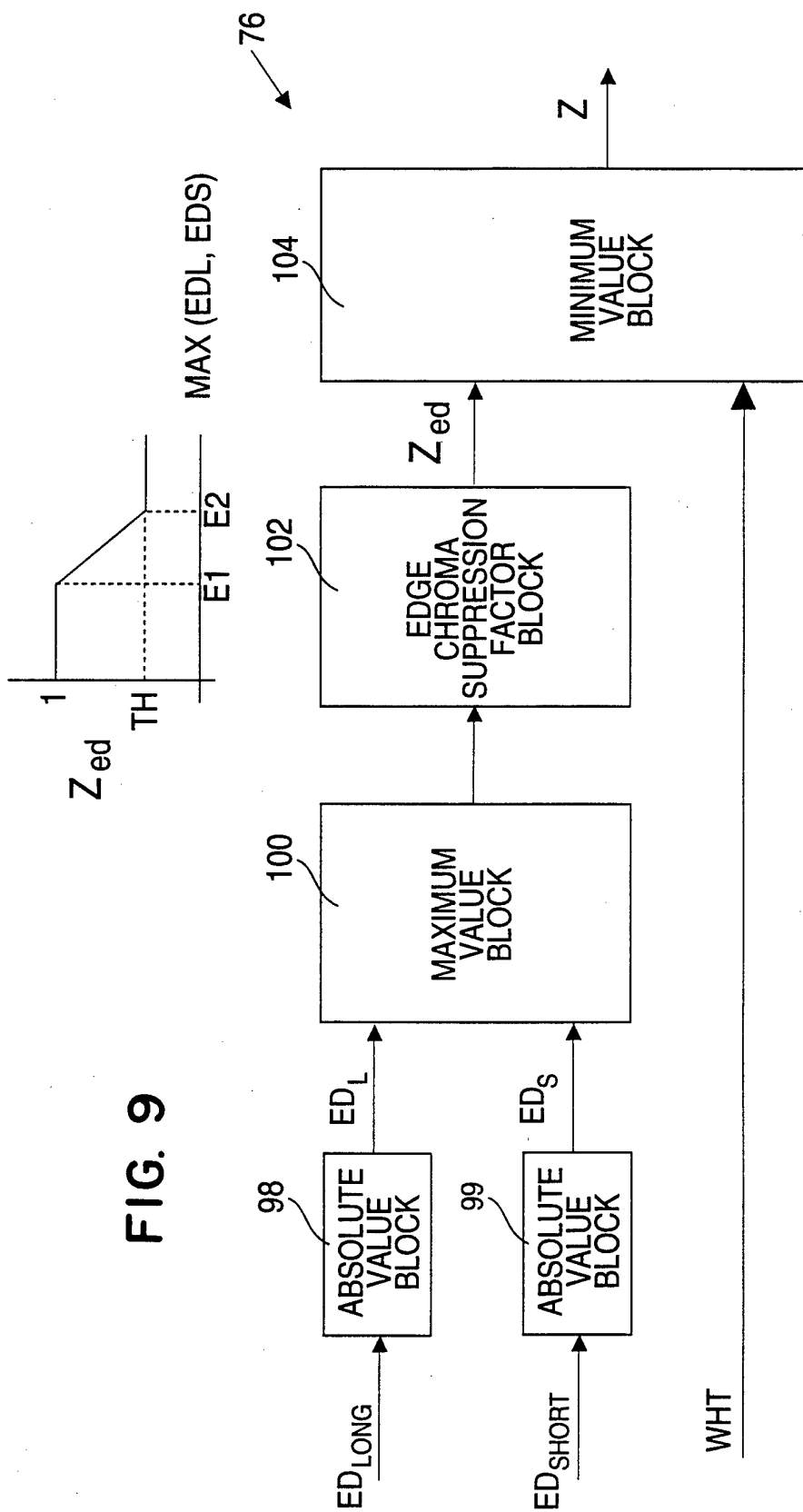


FIG. 9

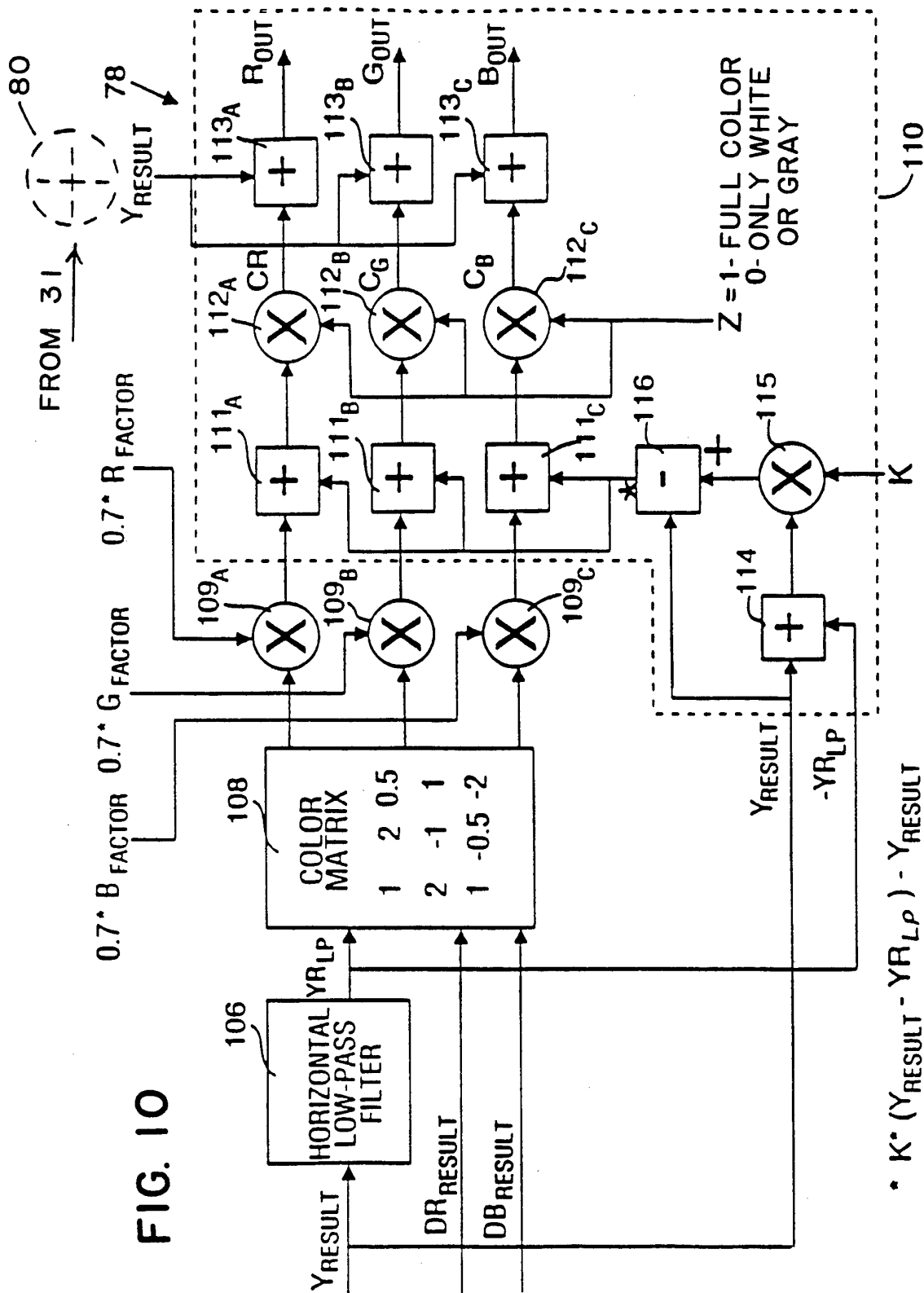


FIG. 10

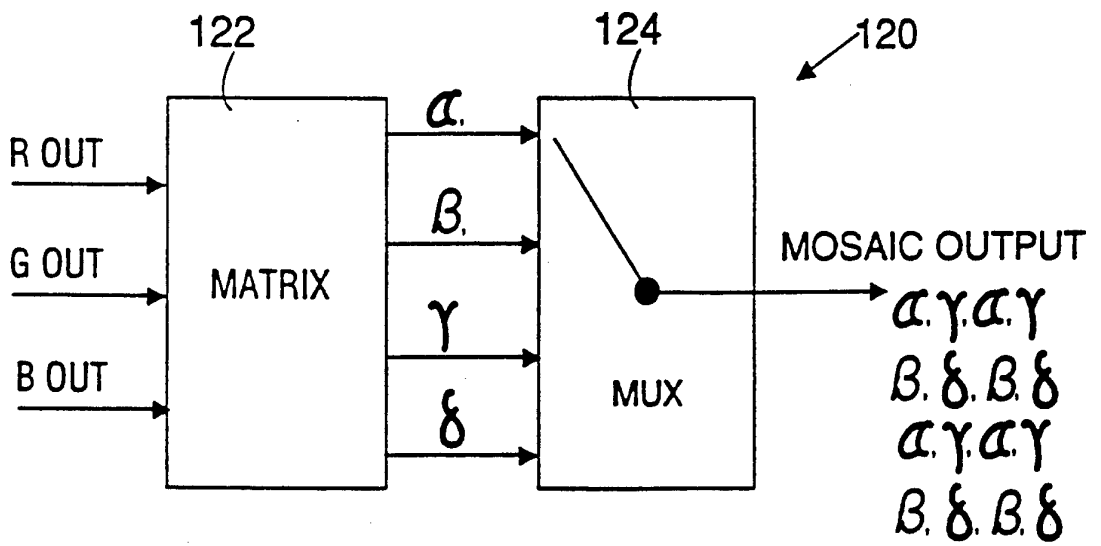


FIG. II

INTERNATIONAL SEARCH REPORT

International application No.  
PCT/US94/01358

A. CLASSIFICATION OF SUBJECT MATTER

IPC(5) : H04N 9/07, 9/04, 5/228  
US CL : 348/234, 276, 228, 253

According to International Patent Classification (IPC) or to both national classification and IPC

B. FIELDS SEARCHED

Minimum documentation searched (classification system followed by classification symbols)

U.S. : H04N 9/07, 9/04, 5/228  
348/223, 228, 229, 234, 253, 266, 272, 279, 276, 362, 630

Documentation searched other than minimum documentation to the extent that such documents are included in the fields searched

Electronic data base consulted during the international search (name of data base and, where practicable, search terms used)

APS

C. DOCUMENTS CONSIDERED TO BE RELEVANT

Category*	Citation of document, with indication, where appropriate, of the relevant passages	Relevant to claim No.
Y	US, A, 4,647,975 (ALSTON et al.) 03 March 1987, Col. 7, lines 49-64, Col. 1, lines 14-16, Col. 4, lines 1 and Col. 6, lines 35-38	1,18,19,20
Y	US, A, 4,614,966 (YUNOKI et al.) 30 September 1986, Figs. 2 and 13	1,4,5,18,19,20
Y	US, A, 4,774,564 (KONISHI) 27 September 1988, see entire document	9,19
A	US, A, 4,584,606 (NAGASAKI) 22 April 1986, see entire document	1-20
A	US, A, 5,138,458 (NAGASAKI et al.) 11 August 1992, see entire document	1-20

Further documents are listed in the continuation of Box C.  See patent family annex.

* Special categories of cited documents:	*T* later document published after the international filing date or priority date and not in conflict with the application but cited to understand the principle or theory underlying the invention
*A* document defining the general state of the art which is not considered to be part of particular relevance	*X* document of particular relevance; the claimed invention cannot be considered novel or cannot be considered to involve an inventive step when the document is taken alone
*E* earlier document published on or after the international filing date	*Y* document of particular relevance; the claimed invention cannot be considered to involve an inventive step when the document is combined with one or more other such documents, such combination being obvious to a person skilled in the art
*L* document which may throw doubts on priority claim(s) or which is cited to establish the publication date of another citation or other special reason (as specified)	*G* document member of the same patent family
*O* document referring to an oral disclosure, use, exhibition or other means	
*P* document published prior to the international filing date but later than the priority date claimed	

Date of the actual completion of the international search 21 March 1994	Date of mailing of the international search report <b>18 APR 1994</b>
--	--

Name and mailing address of the ISA/US Commissioner of Patents and Trademarks Box PCT Washington, D.C. 20231	Authorized officer <i>James J. Grody for</i> SHERRIE HSIA
Facsimile No. NOT APPLICABLE	Telephone No. (703) 305-4738

## INTERNATIONAL SEARCH REPORT

International application No.  
PCT/US94/01358

## C (Continuation). DOCUMENTS CONSIDERED TO BE RELEVANT

Category*	Citation of document, with indication, where appropriate, of the relevant passages	Relevant to claim No.
A	US,A, 4,858,014 (ZEEVI et al.) 15 August 1989 Whole Document	1-20
A	US,A,5,144,442 (GINOSAR et al.) 01 September 1992 Whole Document	1-20
A,P	US, A, 5,247,366 (GINOSAR et al.) 21 September 1993 Whole Document	1-20